Modeling air temperature through a combination of remote sensing and GIS data

J. Cristóbal,[1] M. Ninyerola,[2] and X. Pons[1,3]

[1] Air temperature is involved in many environmental processes such as actual and potential evapotranspiration, net radiation and species distribution. Ground meteorological stations provide important local data of air temperature, but a continuous surface for large and heterogeneous areas is also needed. In this paper we present a hybrid methodology between Remote Sensing and Geographical Information Systems to retrieve daily instantaneous, mean, maximum and minimum air temperatures (2002–2004) as well as monthly and annual mean, maximum and minimum air temperatures (2000–2005) on a regional scale (Catalonia, northeast of the Iberian Peninsula) by means of multiple regression analysis and spatial interpolation techniques. To perform multiple regression analysis we have used geographical and multiresolution remotely sensed variables as predictors. The geographical variables we have included are altitude, latitude, continentality and solar radiation. As remote sensing predictors, we have selected those variables that are most closely related with air temperature such as albedo, land surface temperature (LST) and NDVI obtained from Landsat-5 (TM), Landsat-7 (ETM+), NOAA (AVHRR) and TERRA (MODIS) satellites. The best air temperature models are obtained when remote sensing variables are combined with geographical variables: averaged R^2 = 0.60 and averaged root mean square error (RMSE) = 1.75°C for daily temperatures, and averaged R^2 = 0.86 and averaged RMSE = 1.00°C for monthly and annual temperatures. The results also show that combined models appear in a higher frequency than only geographical or only remote sensing models (87%, 11% and 2% respectively) and that LST and NDVI are the most powerful remote sensing predictors in air temperature modeling.

1. Introduction

[2] Air temperature is a primary descriptor of terrestrial environment conditions all over the Earth and is involved in many important ecological processes such as actual and potential evapotranspiration, net radiation or species distribution [*Idso*, 1981; *Kustas*, 1996; *Prihodko and Goward*, 1997; *Bastiaanssen et al.*, 1998; *Quattrochi and Luvall*, 2000; *Bonan*, 2002; *Kustas et al.*, 2003; *Cristóbal et al.*, 2005]. Furthermore, air temperature is also involved in land surface temperature atmospheric correction algorithms [*Qin et al.*, 2001] and in the generation of several crop stress indexes such as Stress Degree Day or Crop Water Stress Index [*Jackson et al.*, 1977; *Moran et al.*, 1994]. Health sciences also use air temperature as an important parameter to model vector-borne diseases or to measure the effect of extreme temperatures on mortality [*Florio et al.*, 2004]. In addition, accurate air temperature measurements are needed to diminish error propagation in numerical models when air temperature is an important input parameter [*Burrough and McDonell*, 1998].

[3] Multiple regression analysis using geographical variables such as latitude, longitude and continentality (distance from the sea) as predictors has been a classical approach to modeling air temperature [*Blennow*, 1998; *Ninyerola et al.*, 2000; *Monestiez et al.*, 2001]. However, current archives and the availability of some satellite data such as NOAA AVHRR (covering a period of over 30 years) or TERRA/AQUA MODIS (covering a period of over 6 years) make it possible to combine the geographical approach with remote sensing data using variables related with air temperature such as LST, NDVI or albedo.

[4] Air temperature is determined to a great extent by surface properties that vary in both space and time [*Oke*, 1987] and, therefore, directly responds to local changes in land surface [*Arribas et al.*, 2003]. The addition of remote

[1]Department of Geography, Autonomous University of Barcelona, Cerdanyola del Vallès, Spain.

[2]Unit of Botany, Department of Animal Biology, Plant Biology and Ecology, Autonomous University of Barcelona, Cerdanyola del Vallès, Spain.

[3]Center for Ecological Research and Forestry Applications (CREAF), Cerdanyola del Vallès, Spain.

sensing data (which inherently include information about land surface characteristics in air temperature modeling) allows us to improve our knowledge of the complex spatiotemporal patterns of air temperature, in contrast to models that only include geographical variables or that only do spatial interpolation.

[5] Despite the fact that ground meteorological stations provide important local point data, such as air temperature, which is needed to monitor the ecosystem on a macroscale, their spatial density is highly variable and their distribution is usually not optimal for regional and local applications. However, remote sensing data, due to their high sampling rate and repetitive basis over large and heterogeneous regions, offer us a continuous surface that provides additional information between ground meteorological stations where there is a lack of meteorological data [*Vogt et al.*, 1997].

[6] Most of the studies that use remote sensing variables for air temperature modeling are based on a statistical approach, whereas air temperature modeling techniques based on a physical approach are less frequent due to their complexity [*Sun et al.*, 2005]. The temperature/vegetation index (TVX) has been widely employed to model daily air temperature using NOAA AVHRR images [*Goward et al.*, 1994; *Czajkowski et al.*, 1997, 2000; *Prihodko and Goward*, 1997; *Prince et al.*, 1998; *Chokmani and Viau*, 2006; *Riddering and Queen*, 2006]. TVX assumes that the surface temperature of a closed canopy is equal to the air temperature and was developed from the empirical observation that when LST and NDVI measurements are compared, they generally display a linear and negative correlation [*Prince et al.*, 1998; *Quattrochi and Luvall*, 2000]. In order to obtain air temperature, this methodology fits a linear regression to the LST/NDVI relationship using a mobile convolution matrix of 9 × 9 pixels and extends the regression model established from the meteorological stations to a full canopy [*Quattrochi and Luvall*, 2000]. However, the spatial resolution of the air temperature layer obtained is coarser than the images used to fit the model because the spatial resolution is changed to increase the information used to apply the model [*Prince et al.*, 1998].

[7] Other statistical methodologies establish a linear regression between LST and air temperature. These methodologies offer better spatial resolution of outcome air temperature layers because they do not need to change the spatial resolution. In this way, *Vogt et al.* [1997] used LST obtained from NOAA AVHRR to perform a simple linear regression between daily maximum temperature and LST over a Mediterranean region (Andalusia, in the south of the Iberian Peninsula) and *Recondo and Pérez-Morandeira* [2002] also performed a linear regression to model daily and monthly mean and daily maximum air temperature over an Atlantic region (Asturias, in the north of the Iberian Peninsula). Furthermore, *Florio et al.* [2004] compared multiple regression analysis with kriging interpolation introducing both geographical and remote sensing variables to model daily air temperature by also using LST from NOAA AVHRR satellite and obtaining better results with kriging models.

[8] This paper takes these previous studies into account but also aims to introduce the combination of remote sensing variables with geographical variables together with a long meteorological series and a comparison among the different spatial resolutions of the different air temperature models.

[9] In previous studies [*Ninyerola et al.*, 2000; *Ninyerola et al.*, 2007a, 2007b] we employed an optimal methodology using multiple linear regression to model Iberian Peninsula air temperature and precipitation for monthly and annual periods using only geographical variables. The current study has two main objectives.

[10] (1) To quantify the improvement in adding multi-resolution data obtained from the Landsat, MODIS and NOAA satellites between 2002 and 2004 on a regional scale over a large and heterogeneous area (Catalonia, in the north-east of the Iberian Peninsula) to the classical air temperature models (that only use geographical predictors) in instantaneous (at the time of the satellite overpass) and daily air temperature models using a multiple linear regression approach.

[11] (2) To analyze the role of remote sensing and geographical variables in air temperature modeling using MODIS composites from 2000 to 2005 in the same area and applying the same methodology used for the first objective. In this case, however, only monthly and annual air temperature will be modeled.

2. Study Area

[12] The geographical boundary of the study area corresponds to Catalonia (in the north-east of the Iberian Peninsula) and is defined by the following UTM-31 N coordinates (in km): 260 (minimum X coordinate), 528 (maximum X coordinate), 4489 (minimum Y coordinate), and 4749 (maximum Y coordinate) with a total area of approximately 32,000 km^2 (see Figure 1).

[13] Catalonia is composed by three main vegetation units. The first is the Mediterranean vegetation, which covers most of Catalan surface and is dominated by evergreen forests and shrublands ranging from sea level to 600/900 m. The second is the Eurosiberian vegetation dominated by deciduous broad-leaved forests ranging from 600/900 to 1600 m. The third is the Boreoalpine vegetation dominated by grasslands and mainly located in the Pyrenees and the Montseny mountains, ranging from 1600 to 3200 m [*Nuet et al.*, 1991].

[14] Almost the 38% of the surface of Catalonia is covered by forests (including evergreen forests, deciduous broadleaved forests and mixed forests). Another important category is crops, representing the 34.4% of the surface. The third most abundant cover is shrublands (16.4%) followed by grassland (4%), urban (3 %), inland water (1.6%), and other minor categories such as roads, bare soils, etc. (2.6%) [*Ibàñez and Burriel*, 2006].

[15] The climate of Catalonia is typically Mediterranean, with many hours of sunshine, mild in winter and warm in summer. The Pyrenees and the neighboring areas have a high-altitude climate, with abundant snow and minimum temperatures below 0°C in winter, and annual rainfall above 1000 mm. Along the coast, the climate is mild and temperate with temperatures increasing from north to south, while the rain behaves the opposite gradient. The hinterland has a
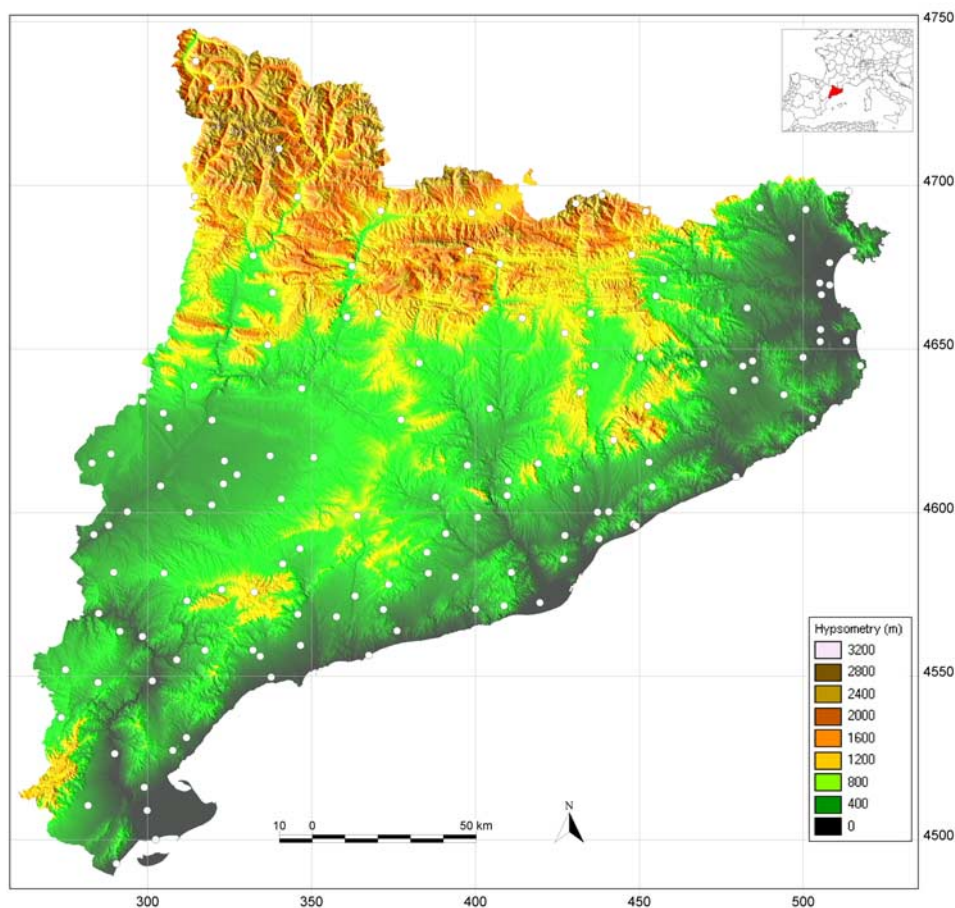
Figure 1. General view of Catalonia, in Universal Transversal Mercator (UTM) projection and geographical location of the filtered meteorological stations from the Catalan Meteorological Service (UTM coordinates are expressed in kilometers).

continental Mediterranean climate, with cold winters and very hot days [*Clavero et al.*, 1996].

3. Material

3.1. Meteorological Data

[16] Half-hourly meteorological data have been downloaded from the Catalan Meteorological Service (SMC) web (meteorological data are available at (http://ww.meteocat.com). SMC currently manages three meteorological ground station networks located in Catalonia. Ground meteorological stations are mainly located in crop areas (64%) but also in natural vegetation (24%) and urban areas (12%). Figure 1 shows the spatial distribution of these three meteorological networks over the study area. The first is the Agroclimatic Network which includes 90 meteorological ground stations mainly covering crop field areas and its height ranges from 0 to 1571 m. The second is the Automatic Station Network which includes 56 automatic meteorological ground stations covering natural vegetation and urban areas, ranging from 0 to 1971 m. The third is the Snow Meteorological Network which includes 8 automatic meteorological ground stations located over grasslands and covering high altitudes from 2200 to 2540 m. From a total of 154 meteorological ground stations corresponding to these three nets we have selected 136 meteorological stations applying a filter criterion con-

sisting in the selection of those stations which have been in service for at least 5 years, a length which is coherent with the remote sensing data used in this study.

3.2. Remote Sensing Data

[17] A set of 52 Landsat images (16 Landsat-5 TM and 36 Landsat-7 ETM+ from path 197 and 198 and rows 31 and 32), 52 NOAA AVHRR images and 52 TERRA MODIS images, between 2002 and 2004 and with a different percentage of cloudiness (ranging from 3% to 35%), have been selected to perform instantaneous and daily multiple regression analysis. Dates have been selected with the aim of covering all months of the year to take into account different daily situations. In addition, in order to compare instantaneous and daily air temperature models using different satellite data we have chosen images of the same date.

[18] To perform monthly and annual multiple regression analysis we have used 8 d and 16 d MODIS composites over the 2000 to 2005 period.

[19] TERRA MODIS images have been downloaded from the EOS Gateway (remote sensing data are available at http://edcimswww.cr.usgs.gov/pub/imswelcome/). We have selected three different types of products which contain the remote sensing variables we have used to perform air temperature modeling: MOD11A1 and MOD11A2 (containing daily and 8 d LST), MOD09GHK and MOD09A1

Table 1. Land Cover Type and Altitude Classes of the Fit (60%) and Test (40%) Meteorological Stations Used in Instantaneous, Daily and Monthly air Temperature Modeling

		Instantaneous and Daily Modeling		Monthly Modeling	
		Fit Stations, %	Test Stations, %	Fit Stations, %	Test Stations, %
Land use type	natural vegetation	22	20	21	19
	crop areas	64	63	62	68
	urban areas	14	17	17	13
Altitude classes, m	0−500	77	71	74	67
	500−1000	18	22	19	26
	1000−1500	4	5	5	5
	>2000	1	2	2	2

(containing daily and 8 d calibrated reflectances) and MOD43B3 (containing 16 d albedo). NOAA AVHRR images products (LST, albedo and NDVI) have been requested from the remote sensing Laboratory of the University of Valladolid (LATUV).

[20] Although image time acquisition is different for each satellite, Landsat and MODIS satellites pass over Catalonia at a similar time, between 9:30 and 11:30 local solar time. On the other hand, NOAA passes over the same area, but between 12:30 and 14:30 local solar time.

4. Methodology

4.1. Regression Model and Model Selection

[21] The methodology that has been applied to retrieve air temperature (T_a) is based on the methodology proposed by *Ninyerola et al.* [2000]. This performs a multiple regression analysis with spatial interpolation of residual errors of ground meteorological station data using only geographical variables as predictors (altitude, latitude, continentality and solar radiation). Spatial interpolation of the residuals has been computed using the Inverse Distance Weighted interpolation because this interpolator offers better results than other methodologies, at least in the case of air temperature modeling [*Ninyerola et al.*, 2000]. This methodology has been applied to produce the Digital Climatic Atlas of the Iberian Peninsula which includes mean, minimum and maximum monthly and annual temperature layers; obtaining a RMSE of less than 1°C in all months [*Ninyerola et al.*, 2007a].

[22] In order to analyze the importance of remote sensing in air temperature modeling we have used a combined approach introducing geographical multiresolution remotely sensed variables as predictors in the multiple regression analysis.

[23] In order to quantify the improvement resulting from the inclusion of remote sensing variables in air temperature modeling, we have also performed multiple regression analysis using only geographical variables.

[24] Model selection has been carried out by means of Mallows' C_p best subsets to select which multiple regression model best describes the data and which variables should be included in the analysis [*Draper and Smith*, 1981]. Mallows' C_p usually performs better than other forward stepwise methods, especially when collinearity is present and it forces the analyst to examine the full model fit, which is the only fit providing accurate standard errors,

error mean square, and *P*-values [*Harrell*, 2001]. All the calculations are based on $\alpha = 0.05$.

[25] As a result of the statistical analysis, resulting models can be classified into three groups depending on their predictors.

[26] (1) *Geographical models*, which only include geographical predictors.

[27] (2) *Remote sensing models*, which only include remote sensing predictors.

[28] (3) *Combined models*, which include both geographical and remote sensing predictors.

4.2. Multiple Regression Variables

[29] The geographical variables we have included are those previously used in other studies [*Ninyerola et al.*, 2000; *Cristóbal et al.*, 2006] such as altitude, latitude, continentality and solar radiation. In these studies, this methodology has been useful to obtain monthly temperature.

[30] The remote sensing predictors we have selected are those variables that could be related with air temperature such as albedo, LST and NDVI. LST and NDVI are often selected as predictors in air temperature modeling literature because of their direct relationship with air temperature [*Goward et al.*, 1994; *Czajkowski et al.*, 1997, 2000; *Prihodko and Goward*, 1997; *Vogt et al.*, 1997; *Prince et al.*, 1998; *Recondo and Pérez-Morandeira*, 2002; *Chokmani and Viau*, 2006; *Cristóbal et al.*, 2006; *Riddering and Queen*, 2006]. Furthermore, we can also suppose that albedo is related with air temperature due to its role in the energy budget.

4.3. Model Validation

[31] For each of the models we have used 60% of the data to fit the multiple regression model and the remaining 40% to test the final model. Table 1 shows the altitude range and the land cover type where the fit and test meteorological ground stations are placed.

[32] The selection of fit and test sets of ground meteorological stations has been done randomly. In monthly and annual air temperature models the same random fit and test sets have been always used. Nevertheless, in the case of instantaneous and daily air temperature modeling, and due to the different level of image cloudiness, we cannot use the same set, which is reflected in Tables 2 and 7, where the number of samples (*n*) is lower. However, in monthly and annual modeling all ground meteorological stations have

Table 2. Mean Air Temperature (T) RMSE and R^2 of Daily Models From 2002 to 2004, Obtained From the Test Set[a]

	T Ins		T Mean		T Min		T Max		n	
	RMSE (°C)	R^2	RMSE (°C)	R^2	RMSE (°C)	R^2	RMSE (°C)	R^2	n Fit, 60%	n Test, 40%
Landsat daily	1.84	0.59	1.35	0.67	2.41	0.46	1.55	0.63	70	42
NOAA daily	1.52	0.61	1.17	0.71	2.12	0.54	1.71	0.67	73	40
MODIS daily	1.93	0.55	1.28	0.66	2.28	0.54	1.82	0.57	70	42
Daily model average	1.76	0.58	1.27	0.68	2.27	0.51	1.69	0.62	71	41

[a]Ins, instantaneous; min, minimum and max, maximum; n fit (60% of meteorological stations), averaged number of stations used to fit all models; n test (40% of meteorological stations), averaged number of stations used to test all models.

been used because is possible to obtain a monthly and annual free cloud image using more images.

[33] Last, we have computed the coefficient of determination (R^2) and the root mean square error (RMSE) for each model.

4.4. Processing of Geographical Variables

[34] Latitude has been approached through the distance of the stations to the Equator because the study area has a small latitudinal range and it is not necessary to use a more precise computation; so we can use the direct UTM-Y coordinate in this case. Altitude has been extracted from a digital elevation model from the Cartographic Institute of Catalonia with 30 m of spatial resolution. Continentality has been defined as the distance from the sea. Finally, instantaneous, daily and monthly solar radiation has been extracted from a potential radiation model proposed by *Pons* [1996].

4.5. Landsat-5 TM and Landsat-7 ETM+ Data Processing

[35] The computation of the Landsat-5 TM and Landsat-7 ETM+ data used in air temperature modeling has been carried out by means of the following methodologies.

[36] (1) *Geometric correction:* images have been corrected using conventional techniques based on first order polynomials taking into account the effect of the relief of the land surface using a Digital Elevation Model [*Palà and Pons*, 1995] obtaining a RMSE of less than 30 m even in the most extreme altitudes. The DEM used to correct the images have a vertical accuracy of 8 m. The spatial resolution of Landsat-7 ETM+ and Landsat-5 TM bands has been resampled to Landsat-5 TM thermal band spatial resolution, 120 m, by means of nearest neighbor resampling.

[37] (2) *Radiometric correction (nonthermal bands):* radiometric correction has been carried out following the methodology proposed by *Pons and Solé-Sugrañes* [1994] which allows us to reduce the number of undesired artifacts that are due to the effects of the atmosphere or to differential illumination which is, in turn, due to the time of the day, the location on the Earth and the relief (some zones are more illuminated than others, cast shadows, etc). Conversion from digital numbers to radiances has been carried out by means of image header parameters taking into account the considerations put forward by *Cristóbal et al.* [2004].

[38] (3) *LST:* due to the lack of atmospheric profiles at satellite pass in Catalonia to compute Landsat-7 ETM+ and Landsat-5 TM thermal band atmospheric correction by means of MODTRAN [*Kneisys et al.*, 1995], thermal band has only been corrected by emissivity effects according to

the methodology proposed by *Hurtado et al.* [1996] and *Valor et al.* [2000]. Apparent brightness temperature used in the LST retrieval has been computed using the methodology proposed by *Markham and Barker* [1986] and *Irish* [2003] for Landsat-5 TM and Landsat-7 ETM+, respectively, using the conversion parameters included in the original image metadata. Emissivity has been computed following the methodology proposed by *Valor and Caselles* [1996]. This methodology calculates surface emissivity values by means of the NDVI-emissivity relation [*van de Griend and Owe*, 1993] and field and laboratory emissivity values [*Salisbury and D'Aria*, 1992].

[39] (4) *Albedo:* broadband albedo has been calculated following the methodology proposed by *Dubayah* [1992] by means of a weighted sum of visible, near infrared and medium infrared bands (1, 2, 3, 4, 5, 7 Landsat-5 TM and Landsat-7 ETM+ bands) using the radiometrically corrected images.

[40] (5) *Cloud removal:* this has been carried out using the methodology proposed by *Cea et al.* [2005]. This methodology is based on an automatic detection of clouds and cloud shadows for Landsat-7 ETM+ and Landsat-5 TM images. Cloud shadows are discriminated by an ISODATA classification (unsupervised classification proposed in 1973) while clouds are detected by means of the response on the thermal band and by several filters based on *Irish* [2000] methodology but including an albedo filter.

4.6. MODIS Data Processing

[41] To compute monthly and annual LST, albedo and NDVI, we have used 8 d LST, 16 d albedo and 8 d calibrated reflectance composites, respectively. MODIS LST composites include both night and day LST which can be useful in minimum and maximum air temperature modeling. Moreover, we have computed a mean LST using night and day data in order to introduce a variable that could be more suitable to perform mean air temperature modeling. Daily albedo has been obtained using daily calibrated reflectance following the methodology proposed by *Liang et al.* [1999]. Daily NDVI has been computed using daily calibrated reflectances.

4.7. NOAA Data Processing

[42] NOAA AVHRR LST, albedo and NDVI images have been requested from the Remote Sensing Laboratory of the University of Valladolid (LATUV) and from the Centre of Reception, Processing, Archiving and Dissemination of Earth Observation Data (CREPAD). Images have been corrected geometrically by means of a hybrid methodology using ground control points and orbital parameters.

Atmospheric correction has been carried out following *Justice et al.* [1991] and *Vermote et al.* [1997] methodologies. Last, LST temperature has been computed by using a split-window algorithm [*Sobrino et al.*, 1991].

5. Results and Discussion

[43] This section is organized according to the air temperature modeling period: daily (instantaneous and daily air temperature modeling) or monthly and annual. Thus we have aggregated daily models and monthly models separately including, in each section, instantaneous (only in daily results), mean, minimum and maximum temperature results. In order to explain the behavior of different daily air temperatures, we have monthly aggregated daily results for the period between 2002 and 2004.

[44] In sections 5.1, 5.2, 5.3, and 5.4 we present the results concerning to the quantification of the improvement in adding multiresolution remote sensing data to the classical models (geographical models). In sections 5.5 and 5.6 we analyze the role of remote sensing and geographical variables in air temperature modeling.

5.1. Predictor Selection

[45] In section 4.1 we have noted that as a result of the model selection analysis predictors are grouped in geographical models, remote sensing models or combined models. The results obtained using Mallows' C_p model selector in daily, monthly and annual air temperature modeling show that models combining remote sensing and geographical predictors (combined models) are statistically selected in a higher frequency than only geographical or only remote sensing models (87%, 11% and 2%, respectively, for the whole set of models). Therefore remote sensing variables have been shown to improve air temperature modeling and are statistically significant in 89% of the models.

[46] In the case of daily models this percentage is similar obtaining 86.4% of combined models, 11.4% of geographical models and 2.2% of remote sensing models, respectively. Therefore these results show that are some days in which remote sensing variables do not improve the models and only geographical variables are selected. On the other hand, although in a minor percentage, there are some days in which geographical variables are not statistically significant and only remote sensing models are selected.

[47] In the case of monthly and annual air temperature modeling all models include geographical and remote sensing predictors.

[48] To quantify the improvement in the addition of remote sensing variables to daily and monthly air temperature models that only use geographical variables, only combined and remote sensing models have been taken into account. Moreover, in order to assess map accuracy in daily models we have averaged the R^2 and the RMSE of the test set (40% of the meteorological stations).

5.2. Daily Models

[49] Table 2 shows daily results of instantaneous, mean, minimum and maximum air temperature modeling for Landsat, MODIS and NOAA cases. Best mean daily air temperature models are obtained when remote sensing variables are combined with geographical variables: averaged test $R^2 = 0.68$ and averaged RMSE = 1.27°C. However, in all cases, minimum and maximum air temperature offer worse results than mean air temperature due to the fact that extreme values are often more difficult to predict than mean values.

[50] Figures 2, 3, 4, and 5 shows monthly mean RMSE for instantaneous, mean, minimum and maximum daily air temperature modeling from 2002 to 2004. Mean RMSE of modeled temperatures range between 1.47°C and 2.17°C, 0.91°C and 1.69°C, 1.72°C and 2.64°C, 1.3°C and 2.36°C in instantaneous, mean, minimum and maximum cases, respectively. Although in daily minimum and maximum cases the RMSE pattern is not clear, in daily instantaneous and mean cases, winter months seem to present higher RMSE values than in other months. This is possibly because the Sun is not so high in the sky so producing a situation more difficult to model (more shadows, lower Lambertian reflection, etc.) on a daily base. However, the number of days analyzed in winter months (10) do not allows us to establish a clear pattern or conclusion.

[51] Tables 3, 4, 5, and 6, show the descriptive statistics for instantaneous, mean, minimum and maximum daily air temperature modeling from 2002 to 2004. Minimum and maximum RMSE values are lower in instantaneous and mean than in minimum and maximum air temperature modeling. This fact also suggests that extreme values are often more difficult to predict than mean values that offer lower RMSE values.

[52] Regarding daily mean temperature, *Goward et al.* [1994], *Czajkowski et al.* [1997, 2000], *Prihodko and Goward* [1997], *Prince et al.* [1998], *Chokmani and Viau* [2006], and *Riddering and Queen* [2006] reported a RMSE ranging from 2.08°C to 5.4°C using TVX methodology. *Recondo and Pérez-Morandeira* [2002] reported a mean RMSE of 2.2°C using a simple linear regression and *Sun et al.* [2005] obtained a mean RMSE of 3°C at more than 80% of the locations processed using a physical approach.

[53] In the case of daily maximum temperature, *Vogt et al.* [1997] and *Recondo and Pérez-Morandeira* [2002] obtained a RMSE ranging from 2 to 2.6°C using a simple linear regression.

[54] In both cases, our results offer a lower RMSE of 1.27°C in the case of daily mean temperatures and a mean RMSE of 1.69°C in the case of daily maximum temperatures (see Table 2).

[55] Spatial resolution comparison among the different satellites has shown that lower resolution daily air temperature models give better results than the obtained with the high resolution ones (see Figures 3, 4, 5 and 6, and Table 2). This could be explained by the fact that ground meteorological station measures are "buffered" by the air itself and so it is a mixed air temperature beyond the meteorological station. When comparing between similar spatial resolutions, we have found that there are differences between NOAA and MODIS air temperature models: NOAA models always give slightly better results than MODIS models. This can be explained by the fact that noon images could be more representative of air temperature than midmorning images. Furthermore, MODIS only offers better results than Landsat in mean and minimum air temperatures.
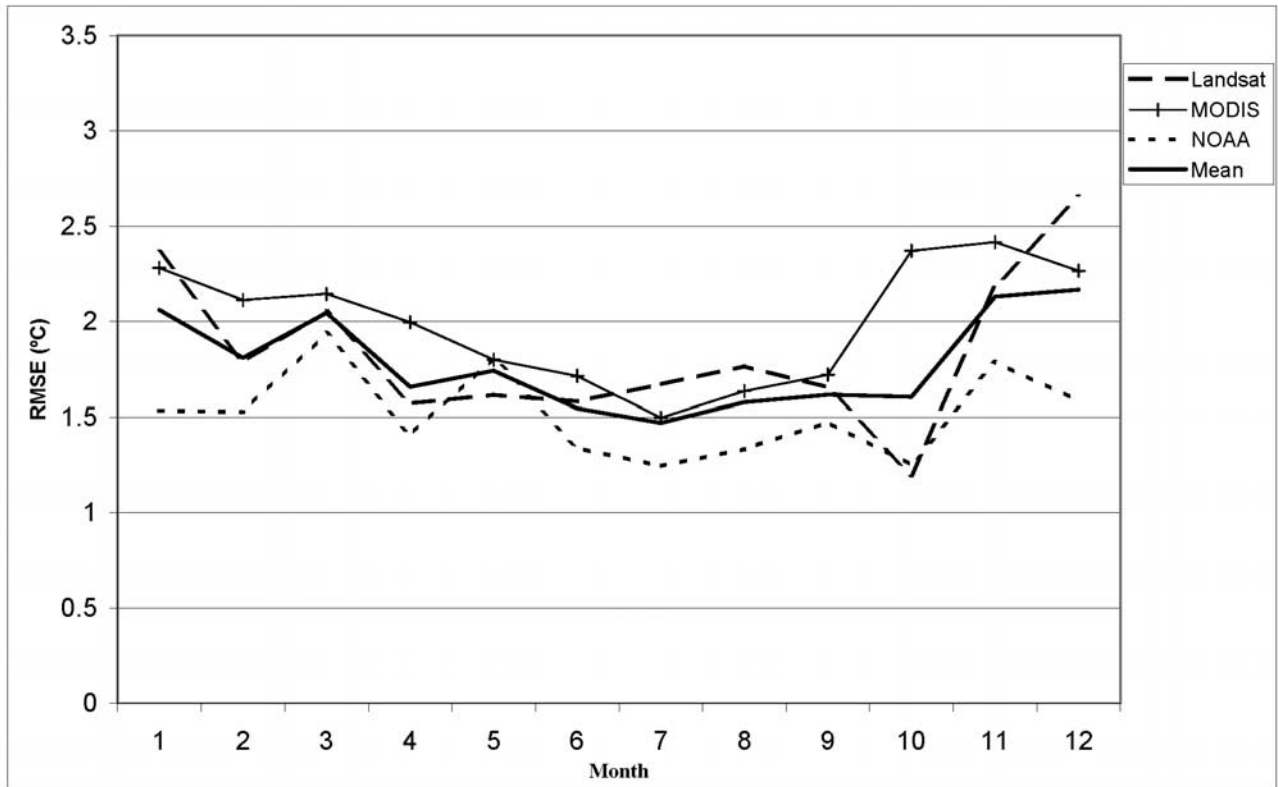
Figure 2. Monthly aggregated RMSE values of instantaneous air temperature modeling from 2002 to 2004. All data computed from 40% of independent meteorological stations (test set).
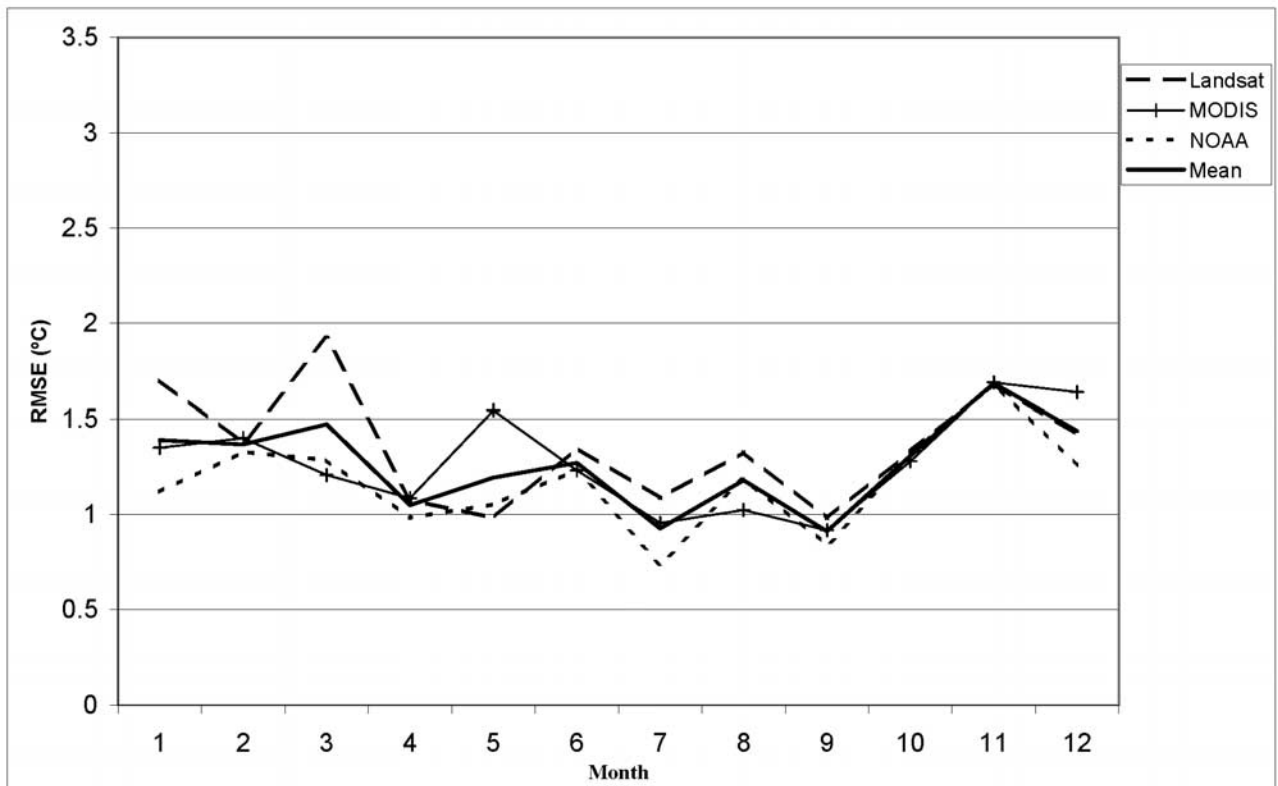

Figure 3. Monthly aggregated values of mean air temperature modeling from 2002 to 2004. All data computed from 40% of independent meteorological stations (test set).
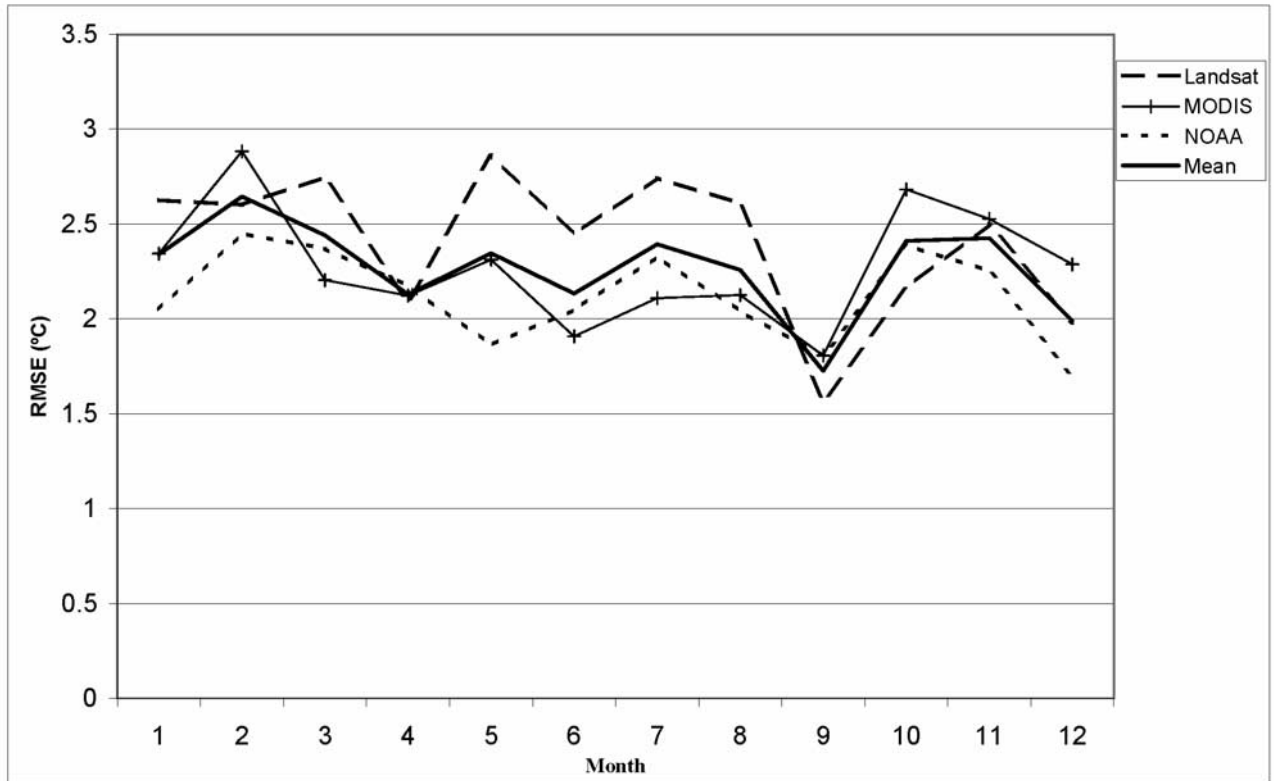
Figure 4. Monthly aggregated RMSE values of minimum air temperature modeling from 2002 to 2004. All data computed from 40% of independent meteorological stations (test set).
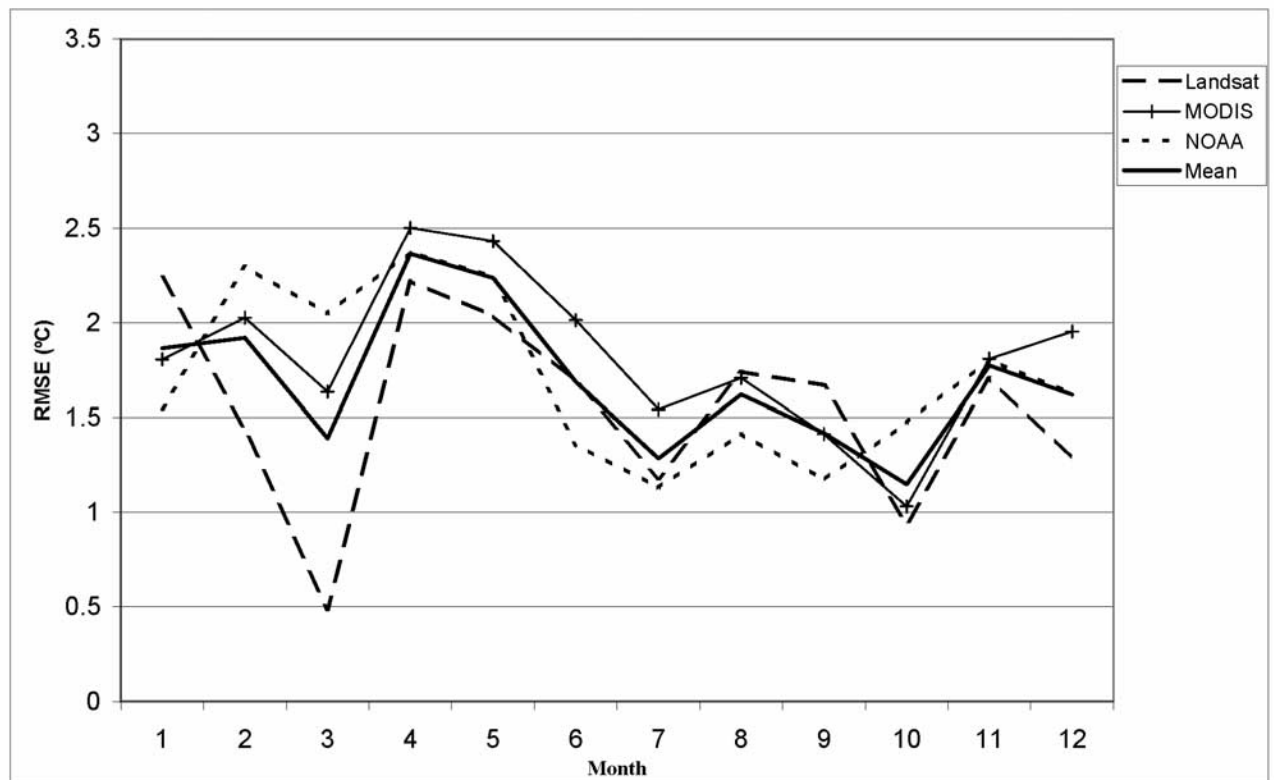

Figure 5. Monthly aggregated RMSE values of maximum air temperature modeling from 2002 to 2004. All data computed from 40% of independent meteorological stations (test set).

Table 3. Descriptive Statistics of Accuracy Measurements of Instantaneous Air Temperature Modeling From 2002 to 2004[a]

T Ins	Min		Max		σ	
	RMSE (°C)	R^2	RMSE (°C)	R^2	RMSE (°C)	R^2
Landsat daily	0.91	0.24	3.09	0.92	0.55	0.21
NOAA daily	0.75	0.23	2.13	0.87	0.33	0.16
MODIS daily	1.06	0.11	2.83	0.82	0.44	0.21
Daily model average	*0.90*	*0.19*	*2.68*	*0.87*	*0.44*	*0.19*

[a]Min, minimum value; max, maximum value; σ, standard deviation. All data computed from 40% of independent meteorological stations (test set).

Table 5. Descriptive Statistics of Accuracy Measurements of Minimum Air Temperature Modeling From 2002 to 2004[a]

T Min	Min		Max		σ	
	RMSE (°C)	R^2	RMSE (°C)	R^2	RMSE (°C)	R^2
Landsat daily	0.99	0.23	3.51	0.74	0.71	0.22
NOAA daily	1.35	0.24	3.14	0.81	0.66	0.20
MODIS daily	1.18	0.24	2.96	0.90	0.65	0.22
Daily model average	*1.17*	*0.24*	*3.20*	*0.82*	*0.67*	*0.21*

[a]Min, minimum value; max, maximum value; σ, standard deviation. All data computed from 40% of independent meteorological stations (test set).

[56] Finally, and because of their low RMSE, these air temperature maps are useful to reduce error propagation in other numerical models that introduce air temperature as an input variable.

5.3. Monthly and Annual Models

[57] Table 7 shows the mean RMSE computed for monthly air temperature models. As in daily models, best mean monthly air temperature models are obtained when remote sensing variables are combined with geographical variables: averaged test R^2 = 0.86 and averaged RMSE = 1.00°C for all monthly temperatures. Furthermore, best results have been obtained when mean LST is introduced instead of night or day LST. For minimum air temperature modeling, best results haven been obtained introducing only night LST, while for maximum temperature modeling, best results have been obtained introducing only day LST. Mean air temperature models present lower mean values of RMSE than minimum and maximum air temperature models and, as we have noted in the case of the daily models, extreme values are often more difficult to predict than mean values, which offer lower RMSE values.

[58] Figure 6 shows the monthly evolution of RMSE for mean, minimum and maximum monthly air temperature modeling from 2000 to 2005. Modeled mean temperatures range between 0.65°C and 0.93°C, 1.06°C and 1.46°C and 0.86°C and 1.30°C for mean, minimum and maximum monthly cases, respectively.

[59] As in the daily case, our results offer a lower mean RMSE of 1.09°C in the case of maximum monthly air temperature modeling (see Table 7) than that reported by *Recondo and Pérez-Morandeira* [2002], who obtained a RMSE of 1.8°C performing a simple linear regression.

[60] Furthermore, as we have noted in the case of the daily air temperature modeling, the low RMSE obtained produces air temperature maps that are useful to reduce error propagation in other numerical models that introduce air temperature as an input variable.

5.4. Analysis of the Inclusion of Remote Sensing Predictors in Classical Air Temperature Modeling

[61] In order to quantify the improvement of the inclusion of remote sensing variables in the classical air temperature modeling, we have also carried out a daily (instantaneous, mean, maximum, and minimum air temperature) and monthly (mean, maximum, and minimum air temperature) modeling using geographical predictors. We have computed geographical models only in daily or monthly models when remote sensing predictors were significant (the 89 % of the analyzed models). Then, we have computed the difference of test RMSE between the *Geographical* models and models that include remote sensing variables (*Combined* and *Remote sensing*).

[62] Table 8 shows these results depending on the remote sensing predictors source (Landsat, NOAA or MODIS) for each one of the analyzed air temperatures (instantaneous, mean, maximum or minimum). A negative value indicates that there has been an improvement in air temperature modeling by the inclusion of remote sensing variables in the model. In 75% of the models compared, best air temperature results have been obtained when remote sensing predictors were present. All values obtained are negative and the difference with regard to the geographical models are around 0.1°C. *Florio et al.* [2004] also reported an improvement of 0.06°C in daily mean air temperature modeling when remote sensing variables were introduced in the analysis.

Table 4. Descriptive Statistics of Accuracy Measurements of Mean Air Temperature Modeling From 2002 to 2004[a]

T Mean	Min		Max		σ	
	RMSE (°C)	R^2	RMSE (°C)	R^2	RMSE (°C)	R^2
Landsat daily	0.65	0.20	2.07	0.96	0.49	0.25
NOAA daily	0.72	0.26	1.70	0.90	0.47	0.20
MODIS daily	0.69	0.27	2.09	0.95	0.46	0.24
Daily model average	*0.69*	*0.24*	*1.95*	*0.94*	*0.47*	*0.23*

[a]Min, minimum value; max, maximum value; σ, standard deviation. All data computed from 40% of independent meteorological stations (test set).

Table 6. Descriptive Statistics of Accuracy Measurements of Maximum Air Temperature Modeling From 2002 to 2004[a]

T Max	Min		Max		σ	
	RMSE (°C)	R^2	RMSE (°C)	R^2	RMSE (°C)	R^2
Landsat daily	0.77	0.23	2.35	0.94	0.79	0.25
NOAA daily	0.78	0.24	3.20	0.93	0.75	0.25
MODIS daily	0.73	0.23	3.99	0.91	0.79	0.27
Daily model average	*0.76*	*0.23*	*3.18*	*0.93*	*0.78*	*0.26*

[a]Max, maximum value; σ, standard deviation. All data computed from 40% of independent meteorological stations (test set).
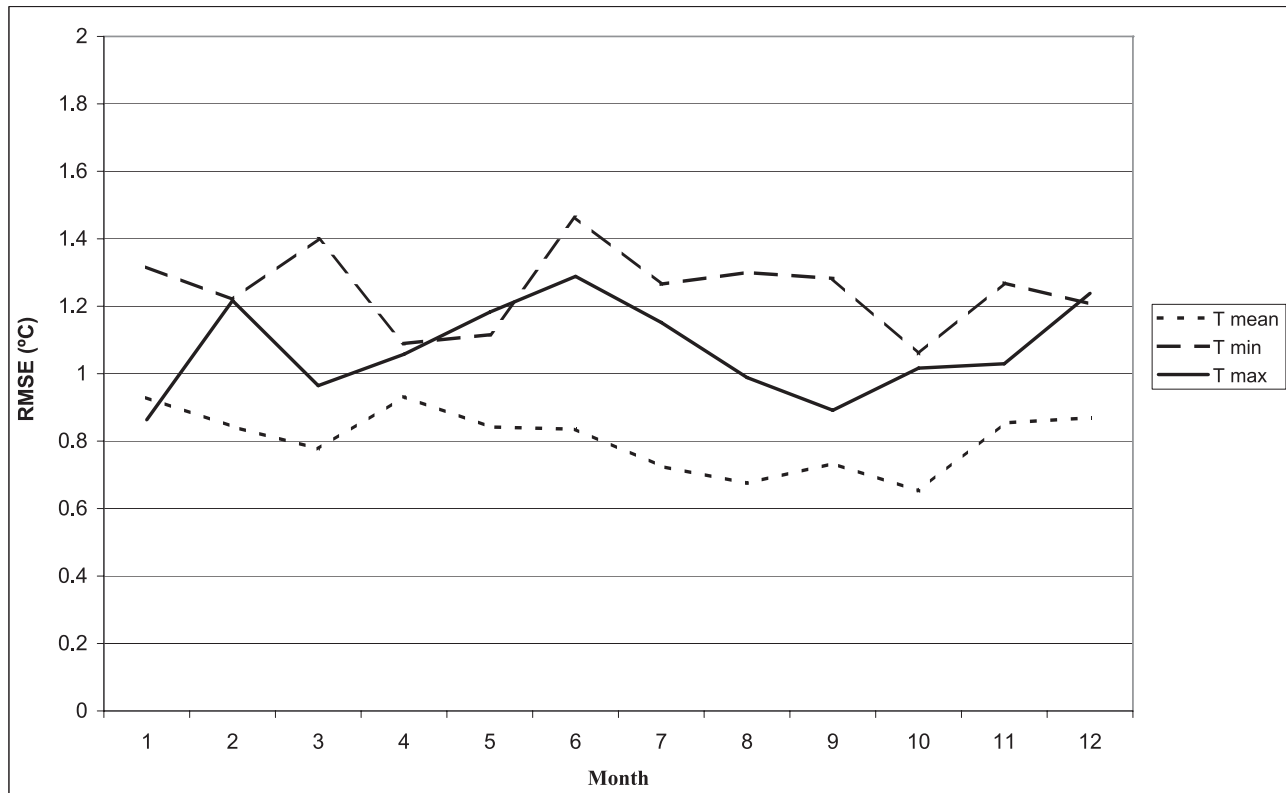
Figure 6. Mean air temperature RMSE of monthly models (MODIS) from 2000 to 2005. min: minimum and max: maximum. All data computed from 40% of independent meteorological stations (test set).

[63] Despite the fact that the improvement of air temperature modeling using remote sensing variables is modest, it should be taken into account that including remote sensing variables in air temperature modeling gives more robust models than only including geographical predictors, according to the Mallows' C_p results in our study. This is consistent with *Oke* [1987], that asserts that air temperature is strongly determined by surface properties, which are included in remote sensing variables but not in geographical variables. In addition, it should be noted that the improvement in monthly models is greater than in daily models because of the length of the meteorological series analyzed.

[64] Daily instantaneous air temperature differences display higher values of difference followed by mean, maximum and minimum air temperature differences because daily instantaneous air temperature correlates better with remote sensing images that are taken at the same time. Daily mean and maximum differences are higher than minimum ones. This can be explained by the fact that minimum temperatures usually occur during the night, when no remote sensing variables have been selected. In this case we have used night LST which has improved minimum air temperature modeling results compared with daily mean and maximum air temperature models.

5.5. Statistical Significance of the Predictors

[65] Regarding the percentage of significant variables in combined models, these behave differently depending on

Table 7. Descriptive Statistics of Accuracy of Monthly and Annual Air Temperature (T) Modeling Using MODIS Data From 2000 to 2005, Obtained From the Test Set Min[a]

	T Mean		T Min		T Max		n	
	RMSE, (°C)	R^2	RMSE, (°C)	R^2	RMSE, (°C)	R^2	n fit, 60%	n test, 40%
Monthly mean	0.78	0.90	1.22	0.78	1.09	0.79	82	54
Monthly min	0.65	0.75	1.06	0.65	0.86	0.67	82	54
Monthly max	0.93	0.94	1.46	0.83	1.29	0.85	82	54
Monthly σ	0.09	0.05	0.13	0.09	0.13	0.08	82	54
Annual	0.78	0.92	1.1	0.85	1.02	0.89	82	54

[a]Minimum; max, maximum; σ, standard deviation; n fit (60% of meteorological stations), averaged number of stations used to fit all models; n test (40% of meteorological stations), averaged number of stations used to test all models.

Table 8. Mean of the Test Set RMSE Differences Between *Geographical Models* and Models That Include Remote Sensing Predictors (*Combined* and *Remote Sensing*) in Daily (From 2002 to 2004) and Monthly (From 2000 to 2005) Cases[a]

°C	T Ins	T Mean	T Min	T Max
Landsat daily	−0.11	−0.07	−0.01	−0.07
NOAA daily	−0.16	−0.11	−0.01	−0.10
MODIS daily	−0.18	−0.11	−0.04	−0.10
Daily model average	*−0.15*	*−0.10*	*−0.02*	*−0.09*
MODIS monthly		−0.10	−0.10	−0.13

[a]Results are grouped depending on the remote sensing predictor satellite. Ins, instantaneous; min, minimum and max, maximum.
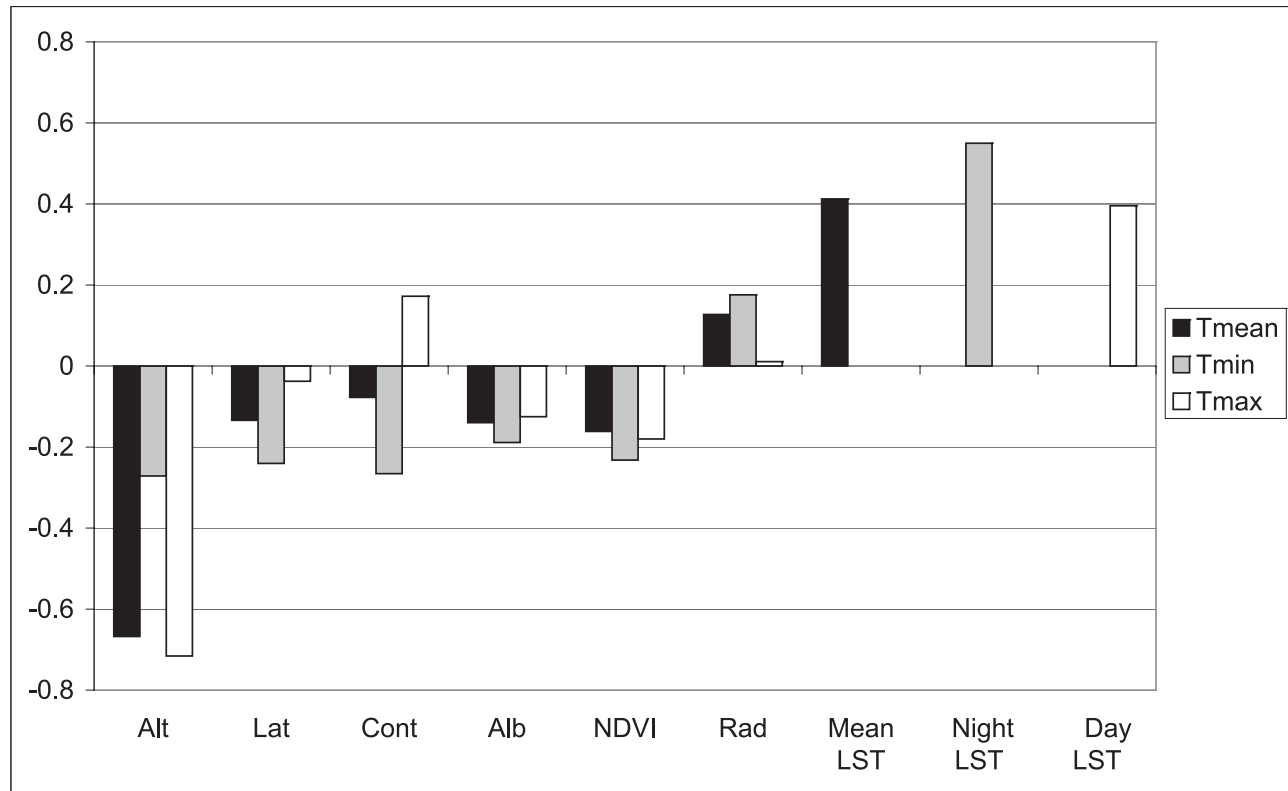
Figure 7. Average of geographical and remote sensing multiple regression beta weights in the case of monthly models (MODIS) from 2000 to 2005 for monthly mean, minimum and maximum air temperature modeling.

time resolution (daily, monthly and annual). In the case of geographical variables, altitude and continentality are the most important variables (included in 79% and 67% of the models, respectively) followed by latitude and solar radiation (included in 55% and 32% of the models respectively) for daily models. In the case of monthly models, continentality and altitude are the most important variables (included in 87% and 71% of the models, respectively) followed by solar radiation and latitude (included in 39% of the models in both cases). However, in other studies [*Ninyerola et al.*, 2000; *Cristóbal et al.*, 2006] altitude usually appears in a higher frequency than continentality but an increase in the meteorological series length would probably change this behavior making it similar to previous studies.

[66] In the case of remote sensing variables for daily models, LST is the most important variable followed by albedo and NDVI (included in 73%, 43% and 41% of the models, respectively). For monthly and annual models, LST and NDVI are the most important variables followed by albedo (included in 77%, 77% and 64% of the models, respectively).

5.6. Multiple Regression Beta Weights

[67] Standardized beta, or beta weight, estimate the relative predictive power of predictors and help to assess the unique importance of the independent variables relative to a given multiple regression model [*Sokal and Rohlf*, 1997]. Because of the lower interpretability of beta weights in daily models, we have only considered monthly air temperature models to analyze beta weight behavior. In order to estab-

lish the relative predictive importance of the independent variables in monthly air temperature modeling we have averaged the beta weights for the different predictors depending on the type of air temperature modeled.

[68] Figure 7 shows the averaged weights of the predictors for the MODIS air temperature modeling from 2000 to 2005.

5.6.1. Geographical Predictor Beta Weights

[69] In previous studies in the Iberian Peninsula [*Ninyerola et al.*, 2000, 2007a] we found the same pattern in the case of altitude and continentality. Altitude has a negative sign in all months and in all types of temperature modeled because air temperature usually decreases as altitude increases. Continentality has a positive sign for all months in maximum air temperature models and a negative sign in minimum air temperature models. In the case of mean temperature models, it is positive in spring and summer months (when the interior is hotter) and negative in winter and autumn months (when the interior is colder). In the work of *Ninyerola et al.* [2000] and *Ninyerola et al.* [2007a] latitude was always found to be positive and this difference can be explained by the fact that in these studies we analyzed longer series of meteorological series instead of only those covering a period of 5 years. Regarding solar radiation, this predictor is always positive in the whole set of air temperature models when it is statistically significant.

[70] With regard to the relative predictive power of geographical predictors, altitude is the most powerful predictor followed by continentality, latitude and solar radia-

tion, in that order. Solar radiation, however, could be more predictive if meteorological stations were located on slopes and not mainly in planes and hills, as they are.

5.6.2. Remote Sensing Predictor Beta Weights

[71] Beta weights of remote sensing predictors are rarely dealt with in the literature and their comparison with other results is often not possible. Albedo always has a negative sign in all air temperature models, so air temperature decreases as albedo increases. Low albedo surfaces absorb heat and increase the air temperature in comparison with the surrounding area. On the other hand, high albedo surfaces reflect incoming solar radiation in a higher proportion and, therefore, decrease the air temperature of the surrounding area. NDVI always displays negative values so air temperature decreases as NDVI values increase. We can relate NDVI with water availability; thus, nonstressed vegetation or well irrigated crops tend to display higher NDVI values than bare soils or stressed vegetation that usually displays lower NDVI values. Because of leaf cooling caused by the usage of visible radiation for photosynthesis and to plant transpiration, vegetation reduces its temperature below air temperature [*Curtis*, 1936; *Pallas et al.*, 1967; *Gates*, 1980], therefore, an increase in NDVI is usually followed by a decrease in air temperature. LST always has a positive sign so air temperature increases as LST increases. Emissive natural covers usually transfer heat to the atmosphere by convection which depends on the ascent of warm air above heated surfaces or the descent of cold air below cooled surfaces [*Monteith and Unsworth*, 1990] as in areas mainly covered by snow or ice. Regarding the different LST predictors, night LST in minimum air temperature modeling shows higher weight than mean or day LST or altitude, which indicates that this predictor is necessary in the case of extreme temperature modeling such as minimum temperature (see Figure 7).

[72] Regarding the relative predictive power of remote sensing predictors, LST is the most powerful predictor followed by NDVI and albedo. Although NDVI and albedo weights are similar, NDVI appears as a significant predictor in a higher proportion than albedo (77% and 64%, respectively).

[73] Finally, it is interesting to note that altitude and LST are the most important predictors of air temperature modeling and that their weights are similar. Besides, both predictors are statistically significant in a higher proportion (71% in the case of altitude and 77% in the case of LST). This means that these two predictors are likely to be used in air temperature modeling in the future.

6. Conclusions

[74] Models combining remote sensing and geographical predictors have been statistically selected more frequently than only geographical (11%) or only remote sensing models (2%) and are statistically significant in 87% of the daily and monthly and annual air temperature models. Moreover, the inclusion of satellite variables has decreased the RMSE, especially in monthly air temperature models, although modest results have been obtained compared with only geographical models.

[75] The obtained RMSE of daily and monthly air temperature combined models has been shown to be moderately accurate in the daily case and highly accurate in the monthly case for all resolutions, especially in instantaneous and mean air temperature modeling. Furthermore, these results suggest that daily and monthly air temperature maps should be introduced as input variables, for example in ecological modeling, because of the low RMSE obtained.

[76] Remote sensing variables have shown themselves to be robust predictors of air temperature, especially LST and NDVI. In the case of remote sensing variables for daily models, LST is the most important variable followed by albedo and NDVI, while in the case of monthly and annual models, LST and NDVI are the most important variables followed by albedo.

[77] Regarding spatial resolution, low spatial resolution images have given better results than those with high spatial resolution when the time the satellite passes is appropriate, due to the fact that ground meteorological station measures the mixed air temperature beyond the point itself.

References

Arribas, A., C. Gallardo, M. A. Gaertner, and M. Castro (2003), Sensitivity of the Iberian Peninsula climate to a land degradation, *Clim. Dyn.*, *20*, 477–489.

Bastiaanssen, W. G. M., M. Meneti, R. A. Feddes, and A. A. M. Holtslag (1998), A remote sensing surface energy balance algorithm for land (SEBAL). I: Formulation, *J. Hydrol.*, *212–213*, 198–212.

Blennow, K. (1998), Modelling minimum air temperature in partially and clear felled forests, *Agric. Meteorol.*, *91*, 223–235.

Bonan, G. B. (2002), *Ecological Climatology: Concepts and Applications*, Cambridge Univ. Press, New York.

Burrough, P. A., and R. A. McDonnell (1998), *Principles of Geographical Information Systems*, Oxford Univ. Press, New York.

Cea, C., J. Cristóbal, and X. Pons (2005), Mejoras en la detección semi-automática de nubes y sombras en imágenes Landsat, paper presented at XI Congreso Nacional de Teledetección, Tenerife, Spain, pp. 359–362, September, Asociación Española de Teledetección.

Chokmani, K., and A. A. Viau (2006), Estimation de la température de l'air et de la quantité de la vapeur d'eau atmosphérique à l'aide des données AVHRR de NOAA, *Can. J. Remote Sens.*, *32*, 1–14.

Clavero, P., J. Martín Vide, and J. M. Raso Nadal (1996), *Atles climàtic de Catalunya. Termopluviometria*, Generalitat de Catalunya (Departament de Política Territorrial i Obres Públiques), Institut Cartogràfic de Catalunya and Departament de Medi Ambient, Barcelona.

Cristóbal, J., X. Pons, and P. Serra (2004), Sobre el uso operativo de Landsat-7 ETM+ en Europa, *Rev. de Teledetec.*, *21*, 55–59.

Cristóbal, J., X. Pons, and M. Ninyerola (2005), Modelling actual evapotranspiration in Catalonia (Spain) by means of remote sensing and geographical information systems, *Gött. Geogr. Abh.*, *113*, 144–150.

Cristóbal, J., M. Ninyerola, X. Pons, and M. Pla (2006), Improving air temperature modelization by means of remote sensing variables, paper presented at 26th IEEE IGARSS Symposium, Denver, Colorado, pp. 2251–2254, July–August, doi:10.1109/IGARSS.2006.582.

Curtis, O. F. (1936), Transpiration and the cooling of leaves, *Am. J. Bot.*, *23*, 7–10.

Czajkowski, K. P., T. Mulhern, S. N. Goward, J. Cihlar, R. O. Dubayah, and S. D. Prince (1997), Biospheric environmental monitoring at BOREAS with AVHRR, *J. Geophys. Res.*, *102*, 29,651–29,662.

Czajkowski, K. P., S. N. Goward, and S. J. Stadler (2000), Thermal remote sensing of near surface environmental variables: Application over the Oklahoma Mesonet, *Prof. Geogr.*, *52*, 345–357.

Draper, N., and H. Smith (1981), *Applied Regression Analysis, Wiley Series in Probability and Mathematical Statistics*, 2nd ed., John Wiley, Hoboken, N. J.

Dubayah, R. (1992), Estimating net solar radiation using Landsat Thematic Mapper and digital elevation data, *Water Resour. Res.*, 28, 2469–2484.

Florio, E. N., S. R. Lele, Y. C. Chang, R. Sterner, and G. E. Glass (2004), Integration AVHRR satellite data and NOAA ground observations to predict surface air temperature: A statistical approach, *Int. J. Remote Sens.*, 25, 2979–2994.

Gates, D. M. (1980), *Biophysical Ecology*, Springer, New York.

Goward, S. N., R. H. Waring, D. G. Dye, and J. Yang (1994), Ecological remote sensing at OTTER: Satellite macroscale observations, *Ecol. Appl.*, 4, 322–343.

Harrell, F. E. (2001), *Regression Modeling Strategies. With Applications to Linear Models, Logistic Regression Models and Survival Analysis*, 568 pp., Springer, New York.

Hurtado, E., A. Vidal, and V. Caselles (1996), Comparison of two atmospheric correction methods for Landsat TM thermal band, *Int. J. Remote Sens.*, 17, 237–247.

Ibàñez, J. J., and J. A. Burriel (2006), MCSC: A high-resolution thematic digital cartography, paper presented at 5th European Congress on Regional Geoscientific Cartography and Information Systems, Barcelona, Spain, pp. 278–280, June , Institut Cartogràfic de Catalunya, B-31042-2006/2.

Idso, S. B. (1981), A set of equations for full spectrum 8 to 14μm thermal radiation from cloudless skies, *Water. Resour. Res.*, 17, 295–304.

Irish, R. (2000), Landsat 7 automatic cloud cover assessment, paper presented at VI SPIE Algorithms for Multispectral, Hyperspectral, and Ultraspectral Imagery, vol. 4049, Orlando, Florida, pp. 155–166, August.

Irish, R. (2003), Landsat 7 Science Data Users Handbook, NASA, http://ltpwww.gsfc.nasa.gov/IAS/handbook/handbook_toc.html.

Jackson, R. D., R. J. Reginato, and S. B. Idso (1977), Wheat canopy temperature: A practical tool for evaluating water requirements, *Water. Resour. Res.*, 13, 651–656.

Justice, C. O., T. F. Eck, D. Tanré, and B. N. Holben (1991), The effect of water vapour on the Normalized Difference Vegetation Index derived for the Sahelian region from NOAA AVHRR data, *Int. J. Remote Sens.*, 12, 1165–1187.

Kneisys, F. X., et al. (1995), *The MODTRAN 2/3 and LOWTRAN 7 Model*, Ontar Corp., North Andover, USA.241.60.

Kustas, W. P. (1996), Use of remote sensing for evapotranspiration monitoring over land surfaces, *Hydrol. Sci. J.*, 41, 495–516.

Kustas, W. P., A. N. French, J. L. Hatfield, T. J. Jackson, M. S. Moran, A. Rango, J. C. Ritchie, and T. J. Schmugge (2003), Remote sensing research in hydrometeorology, *Photogramm. Eng. Remote Sens.*, 69, 631–646.

Liang, S., A. H. Strahler, and C. Walthall (1999), Retrieval of land surface albedo from satellite observations: A simulation study, *J. Appl. Meteorol.*, 38, 712–725.

Markham, B. L., and J. L. Barker (1986), Landsat MSS and TM postcalibration dynamic ranges, exoatmospheric reflectance and at-satellite temperatures, *EOSAT Landsat Tech. Notes*, 1, 3–8.

Monestiez, P., D. Courault, D. Allard, and F. Ruget (2001), Spatial interpolation of air temperature using environmental context: Application to a crop model, *Environ. Ecol. Stat.*, 8, 297–309.

Monteith, J. L., and M. H. Unsworth (1990), *Principles of Environmental Physics*, 2nd ed., Edward Arnold, London.

Moran, M. S., T. R. Clarke, Y. Inoue, and A. Vidal (1994), Estimating crop water deficit using the relation between surface-air temperature and spectral vegetation index, *Remote Sens. Environ.*, 49, 246–263.

Ninyerola, M., X. Pons, and J. M. Roure (2000), A methodological approach of climatological modelling of air temperature and precipitation through GIS techniques, *Int. J. Climatol.*, 20, 1823–1841.

Ninyerola, M., X. Pons, and J. M. Roure (2007a), Objective air temperature mapping for the Iberian Peninsula using spatial interpolation and GIS, *Int. J. Climatol.*, 27(9), doi:10.1002/joc.1462, 1231–1242.

Ninyerola, M., X. Pons, and J. M. Roure (2007b), Monthly precipitation mapping of the Iberian Peninsula using spatial interpolation tools implemented in a Geographic Information System, *Theor. Appl. Climatol.*, 89(3-4), doi:10.1007/s00704-006-0264-2, 195–209.

Nuet, J., J. M. Panareda, and A. M. Romo (1991), *Vegetació de Catalunya*, 153 pp., Eumo, Barcelona.

Oke, T. R. (1987), *Boundary Layer Climates*, 2nd ed., 435 pp., Routledge, London.

Palà, V., and X. Pons (1995), Incorporation of relief into geometric corrections based on polynomials, *Photogramm. Eng. Remote Sens.*, 61, 935–944.

Pallas, J. E., B. E. Michel, and D. G. Harris (1967), Photosynthesis, transpiration, leaf temperature, and stomatal activity of cotton plants under varying water potentials, *Plant Physiol.*, 42, 76–88.

Pons, X. (1996), Estimación de la Radiación Solar a partir de modelos digitales de elevaciones. Propuesta metodológica, paper presented at VII Coloquio de Geografía Cuantitativa, Sistemas de Información Geográfica y Teledetección, Vitoria-Gasteiz.

Pons, X., and L. Solé-Sugrañes (1994), A simple radiometric correction model to improve automatic mapping of vegetation from multispectral satellite data, *Remote Sens. Environ.*, 47, 1–14.

Prihodko, L., and S. N. Goward (1997), Estimation of air temperature from remotely sensed surface observations, *Remote Sens. Environ.*, 60, 335–346.

Prince, S. D., S. J. Goetz, R. O. Dubayah, K. P. Czajkowski, and M. Thawley (1998), Inference of surface and air temperature, atmospheric precipitable water and vapor pressure deficit using Advanced Very High-Resolution Radiometer satellite observations: Comparison with field observations, *J. Hydrol.*, 212-213, 230–249.

Qin, Z., A. Karnieli, and P. Berliner (2001), A mono-window algorithm for retrieving land surface temperature from Landsat TM data and its application to the Israel-Egypt border region, *Int. J. Remote Sens.*, 22, 3719–3746.

Quattrochi, D. A., and J. C. Luvall (Eds.) (2000), *Thermal Remote Sensing in Land Surface Processes*, CRC Press, Boca Raton, Fla.

Recondo, C., and C. S. Pérez-Morandeira (2002), Obtención de la temperatura del aire en Asturias a partir de la temperatura de la superficie terrestre calculada con imágenes NOAA-AVHRR, *Rev. Teldetec.*, 17, 5–12.

Riddering, J. P., and L. P. Queen (2006), Estimating near-surface air temperature with NOAA AVHRR, *Can. J. Remote. Sens.*, 32, 33–43.

Salisbury, J. W., and D'Aria (1992), Emissivity of terrestrial materials in the 8-14 μm atmospheric window, *Remote Sens. Environ.*, 42, 83–106.

Sobrino, J. A., C. Coll, and V. Caselles (1991), Atmospheric correction for land surface temperature using NOAA-11 AVHRR channels 4 and 5, *Remote Sens. Environ.*, 38, 19–34.

Sokal, R. R., and F. J. Rohlf (1997), *Biometry, The Principles and Practice of Statistics in Biological Research*, 3rd ed., W. H. Freeman, New York.

Sun, Y.-J., J.-F. Wang, R.-H. Zhang, R. R. Gillies, Y. Xule, and Y.-C. Bo (2005), Air temperature retrieval from remote sensing data based on thermodynamics, *Theor. Appl. Climatol.*, 80, 37–48.

Valor, E., and V. Caselles (1996), Mapping land surface emissivity from NDVI: Application to European, African and South American areas, *Remote Sens. Environ.*, 57, 167–184.

Valor, E., V. Caselles, C. Coll, F. Sánchez, E. Rubio, and F. Sospedra (2000), Simulation of a medium-scale-surface-temperature instrument from Thematic Mapper data, *Int. J. Remote Sens.*, 21, 3153–3159.

van de Griend, A. A., and M. Owe (1993), On the relationship between thermal emissivity and the normalized difference vegetation index for natural surfaces, *Int. J. Remote Sens.*, 14, 1119–1131.

Vermote, E. F., D. Tanre, J. L. Deuze, M. Herman, and J.-J. Morcette (1997), Second simulation of the satellite signal in the solar spectrum, 6S: An overview, *IEEE Trans. Geosci. Remote Sens.*, 35, 675–686.

Vogt, J. V., A. A. Viau, and F. Paquet (1997), Mapping regional air temperature fields using satellite-derived surface skin temperatures, *Int. J. Climatol.*, 17, 1559–1579.

————————————

J. Cristóbal, Department of Geography, Letters Faculty, Autonomous University of Barcelona, Cerdanyola del Vallès 08193, Spain. (jordi.cristobal@uab.cat)

M. Ninyerola, Unit of Botany, Department of Animal Biology, Biosciences Faculty, Plant Biology and Ecology, Autonomous University of Barcelona, Cerdanyola del Vallès 08193, Spain.

X. Pons, Center for Ecological Research and Forestry Applications (CREAF), Biosciences Faculty, Autonomous University of Barcelona, Cerdanyola del Vallès 08193, Spain.